# A Combined *in-Situ* PM-RAIRS and Kinetic Study of Single-Crystal Cobalt Catalysts under Synthesis Gas at Pressures up to 300 mbar

**Gerhard A. Beitel,† Cor P. M. de Groot, Heiko Oosterbeek, and Jon H. Wilson***

*Shell Research and Technology Centre, Amsterdam, P.O. Box 38000, 1030 BN Amsterdam, The Netherlands*

*Received: October 28, 1996*[⊗]

The coadsorption behavior of CO and hydrogen on Co(0001) during exposure to mixtures of $H_2$ and CO at pressures up to 300 mbar and temperatures between 298 and 490 K has been studied by *in-situ* polarization modulation reflection absorption infrared spectroscopy (PM-RAIRS). At 490 K it is shown that adsorbed CO molecules attached to cobalt atoms at step edges ("defect sites") disappear. We explain this observation in terms of hydrocarbon formation at defect sites, which blocks the adsorption of CO at these positions. To support this explanation, both *ex-situ* X-ray photoelectron spectroscopy measurements and kinetic measurements have been performed. The kinetic measurements provide direct evidence for a link between the number of defect sites at the surface and the total Fischer−Tropsch activity.

## 1. Introduction

The adsorption and reactivity behavior of coadsorbed CO and hydrogen on the surfaces of group VIII transition metals is of considerable interest in relation to their commercial importance as catalysts for the Fischer−Tropsch (FT) reaction.[1−4] In the FT reaction, a variety of predominantly straight-chain hydrocarbon products are formed from a mixture of CO and $H_2$ (hereafter referred to as synthesis gas or "syngas") at temperatures between 450 and 570 K and pressures typically in the range 5−30 bar. In the case of Fe-, Ru-, and Co-based FT catalysts, and dependent on the exact reaction conditions, linear *n*-paraffins and 1-olefins form the majority products. Despite the considerable research effort which has already been devoted to this particular syngas conversion reaction, a detailed understanding of the coadsorption behavior of CO and hydrogen under representative catalytic conditions has been hampered by the paucity of available *in-situ* experimental techniques. The purpose of this paper is to address the *in-situ* coadsorption and reactivity behavior of CO and hydrogen under FT reaction conditions in the case of a model Co(0001) catalyst surface in some detail, focusing particularly on the role played by surface defects in this complex heterogeneous reaction.

Adsorption studies on cobalt single-crystal surfaces have previously been carried out on the Co(0001),[5−9] Co(10$\bar{1}$2),[10−12] Co(11$\bar{2}$0),[12,13] and Co(10$\bar{1}$0)[14,15] surfaces. The adsorption and dissociation behavior of CO in the absence of $H_2$ has been studied by low-energy electron diffraction (LEED),[5−8,10,11,13−15] ultraviolet photoelectron spectroscopy (UPS),[6,13,14] Auger electron spectroscopy (AES),[5,6,9−14] thermal desorption spectroscopy (TDS),[5,10,11,15], electron energy loss spectroscopy (EELS),[6,9,12−14] work function measurements ($\Delta\phi$),[6,10,11,13,14] and reflection absorption infrared spectroscopy (RAIRS).[15] The coadsorption behavior of CO and $H_2$ has been studied so far on the Co(0001) surface only by TDS,[16] although numerous coadsorption studies have been done on various other transition metal surfaces.[17]

All of the above-mentioned studies were performed under ultrahigh-vacuum (UHV) conditions at CO pressures below $10^{-6}$ mbar. Hence, there is a pressure gap of at least 10 orders of magnitude between these studies and the industrial conditions of the Fischer−Tropsch process. This difference makes conclusions drawn from results obtained under UHV conditions of unknown relevance to industrial catalytic practice.[18−20]

Considerable progress has been made so far by the combination of *ex-situ* UHV analysis with high-pressure sample treatment.[9,12,21−24] Changes in the surface structure of a Co(0001) surface following exposure to synthesis gas in a high-pressure reactor (520 K, 4 bar) and observed by *ex-situ* UHV scanning tunneling microscopy (STM) have been reported by Wilson *et al.*[25] An island structure was shown to develop under Fischer−Tropsch synthesis conditions on an initially atomically flat surface. The development of these islands was believed to be caused by an etch−regrowth process in which cobalt atoms are removed from edge and kink sites under reaction conditions, creating mobile cobalt species on the terraces which subsequently nucleate and form discrete single-atom high cobalt islands. The mobile species were assumed to be cobalt subcarbonyls $Co(CO)_x$ ($x = 1-3$). The presence of such species is known in the case of supported rhodium catalysts[26] as well as on Rh field emitter tips at $10^{-6}$ mbar CO pressure[27] and has also been postulated in the case of single-crystal rhodium surfaces at CO pressures between 1 and 150 mbar.[28]

In order to make the link between structure/composition and catalytic performance, *in-situ* methods have to be used. Unfortunately, there are only a few *in-situ* analysis techniques available which can be applied to characterize catalyst surfaces under high-pressure (and high-temperature) conditions. Reflection absorption infrared spectroscopy (RAIRS) is an *in-situ* technique well-suited for providing information about adsorbate layers (in particular),[29−34] but in the case of CO, the contribution from CO molecules in the gas phase to the absorption spectrum at CO pressures above $10^{-3}$ mbar completely obscures the weak absorption signal of surface-adsorbed CO.[35] It is, however, possible to subtract out the gas phase absorption by coding the surface absorption signal by means of the polarization modulation (PM) technique applied to a conventional RAIR spectrometer. The efficiency of polarization modulation RAIRS (PM-RAIRS) to discriminate near surface absorptions from the isotropic stray absorptions occurring in the gas phase has been demonstrated for both a setup using a dispersive infrared spectrometer and a setup using a Fourier transform spectrometer.[36−39]

Briefly, the basic principle of the PM-RAIRS method used in the present study comprises the combination of a conventional

† Present address: Siemens AG, Semiconductor Division, P.O. Box 81730, D-81739 Munich, Germany.

* Corresponding author.

⊗ Abstract published in *Advance ACS Abstracts,* May 1, 1997.

S1089-5647(96)03337-8 CCC: $14.00 

Fourier transform RAIRS spectrometer (linearly polarized light strikes surface at grazing incidence) with a photoelastic modulator (PEM) which rapidly modulates the polarization state of the incident electric field (ideally between p and s linear states). While p-polarized light produces a net surface electric field which can interact with adsorbed molecules, the net surface electric field in the case of s-polarized light vanishes. Both polarization states are on the other hand equally sensitive to gas phase absorption because gas phase molecules are randomly oriented. By electronic filtering and demodulation (lock-in techniques), a differential reflectivity spectrum is computed, which does not show contributions from the gas phase and which has, compared to the absolute measurement of a conventional RAIRS setup, a much higher surface sensitivity.

In a recent study the PM-RAIRS technique, based on a Fourier transform (FT) RAIR spectrometer, was applied by Beitel *et al.*[40] for the first time for an *in-situ* investigation of model systems for heterogeneous catalysts. The adsorption behavior of CO on Co(0001) surfaces was investigated at pressures up to 600 mbar and temperatures between 300 and 550 K. In that study, it was shown that CO can be used as a probe molecule to investigate changes in surface defect structure and morphology. The influence of surface defects on the adsorption behavior of CO was investigated by comparing an annealed cobalt surface with a sputtered cobalt surface following $Ar^+$ ion bombardment.

In this paper, we present PM-RAIRS studies of the coadsorption behavior of hydrogen and CO on Co(0001) at pressures up to 300 mbar and temperatures in the range 298−490 K. Sputtered surfaces have again been used to examine the influence of defects. In combination with postreaction X-ray photoelectron spectroscopy (XPS) and reactivity measurements, we have now obtained direct evidence for a link between the number of defect sites on Co(0001) and its overall FT activity, as suggested by the earlier STM study.

## 2. Experimental Section

The UHV system in which the PM-RAIRS and XPS experiments were carried out is described elsewhere.[40] The kinetic measurements were performed in a separate UHV system containing a high-pressure reactor (HPR), which can be operated at total pressures in the range 1−20 bar. Samples can be easily transferred between the HPR and UHV for pre- and postreaction analysis. The UHV analysis chamber is similarly equipped with facilities for TPD and XPS as well as for UHV sample preparation. It also contains an STM for detailed examination of local surface structure at the atomic level (used for the experiments described in ref 25).

The HPR is itself a small, internally gold-coated, UHV chamber, which has been modified so as to follow closely the behavior of a continuous ideally stirred tank reactor (CSTR). It has a total volume of 14 mL and contains a heating post for fixing the sample temperature at some preset value. $H_2$ and CO can be controllably premixed and introduced via mass flow controllers (Brooks). Reaction products are analyzed on-line by means of a gas chromatograph (Chrompack 9000) directly coupled to the reactor. For the kinetic measurements, a 2:1 ratio of $H_2$ and CO was introduced with a maximum flow rate of 15 mL/min, while the sample temperature inside the HPR was raised at a heating rate of 4 K/min. Once filled, the flow rate was brought back to a constant value of 1 mL/min. In this way, the sample was brought to a temperature of 523 K under flowing syngas at a total pressure of 1 bar.

The gases used (in either UHV system) were $H_2$, CO, Ar, and $O_2$ and were of 99.995% purity or better. The $H_2$ was additionally cleaned by passing the gas through a palladium diffuser unit before being introduced into our gas handling system. Iron and nickel carbonyls present in the CO gas due to contact with the stainless steel walls of the gas handling lines were decomposed in a trap consisting of a copper pipe heated to 570 K and containing zeolite 3A.

The Co(0001) crystals (10 × 2.5 mm circular disc) were of 99.999% purity and were purchased from Metal Crystals Ltd. The samples were polished down to a level of 1 $\mu$m, with a maximum axial misorientation of ±0.5°. Samples were mounted on a heatable molybdenum or copper sample holder (ESCA stub, Fisons Instruments). Sample temperature was measured by a thermocouple spot-welded to the side of the crystal. For the kinetic measurements, blank experiments were conducted to check that background activity levels (HPR + sample stub) were acceptably low.

Crystals were prepared in UHV by extensive cycles of $Ar^+$ ion sputtering at 620 K (1.0−1.5 kV, $5 \times 10^{-6}$ mbar of Ar, sample current 0.5−1 $\mu$A, 1−18 h) and UHV annealing at the same temperature (10 min). Residual carbon of about 2−4% of a monolayer could be further decreased below 1% of a monolayer by cycles of annealing in $1 \times 10^{-7}$ mbar of $O_2$, in $1 \times 10^{-7}$ mbar of $H_2$, and in vacuum at 620 K as judged by XPS. Following this annealing procedure, a slight oxygen contamination of around 1−2% of a monolayer remained at the surface. In a final annealing step, samples were flashed to ∼950 K, since this is known to produce a stepped surface with large atomically flat terraces and without destroying the integrity of the Co(0001) single crystal[5,25] (hcp → fcc phase transition occurs at ∼673 K). This surface was used for the PM-RAIR and kinetic experiments on an "annealed" surface with a low defect concentration. In later experiments, however, this final annealing step was omitted since it was not found to affect the measured PM-RAIR spectra to a significant extent. By $Ar^+$ ion sputtering the annealed surface at room temperature for 1 h, we produced a highly defective surface for investigating the influence of defects.

## 3. Results

Figure 1a−d shows a sequence of PM-RAIR spectra, in which the CO adsorption behavior of an annealed Co(0001) surface under pure CO and under synthesis gas ($H_2$/CO = 2) is compared. For a given $p_{CO}$, the spectra taken at successively higher pressures under synthesis gas at 298 K are almost identical to the spectra taken under pure CO. In both cases, the main absorption signal at ∼2000−2050 $cm^{-1}$ due to linearly bonded CO[40] shows similar shifts in frequency, with increasing $p_{CO}$, as well as comparable changes in the total peak intensity. Furthermore, at $p_{CO}$ = 100 mbar, the development of a second peak at ∼1900 $cm^{-1}$ due to bridge-bonded CO[40] can be clearly identified in both sets of spectra (Figure 1c).

After raising the temperature to 490 K (typical temperature for Fischer−Tropsch synthesis), the behavior of the main CO absorption signal at ∼2000−2050 $cm^{-1}$ under pure CO, on the one hand, and under synthesis gas, on the other, shows major differences. In the case of pure CO, the main absorption signal shows an increase in overall intensity and a shift to higher frequencies. In addition, an extra peak at 2080 $cm^{-1}$ develops, which has been previously assigned to CO bonded to defects in an earlier publication.[40] In the case of synthesis gas, the only effect of increasing temperature on the main absorption signal is to cause an increase in total peak intensity. The main CO absorption signal under synthesis gas is red-shifted by ∼20 $cm^{-1}$ compared to the situation under pure CO. In both cases, the bridge-bonded signal at ∼1850−1950 $cm^{-1}$ disappears upon raising the temperature.

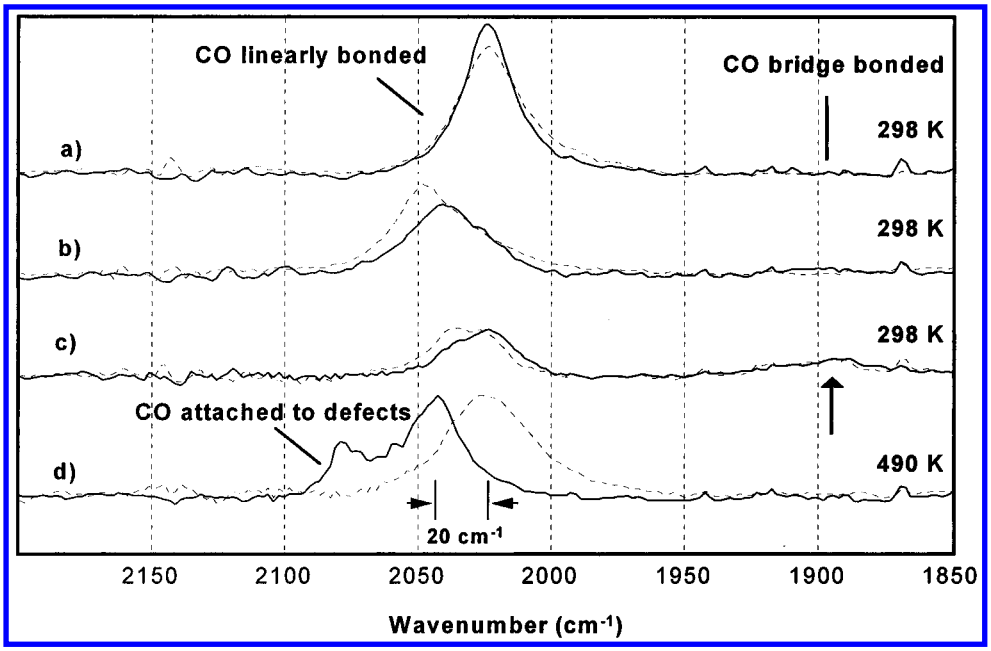


**Figure 1.** Sequence of PM-RAIR spectra taken on an annealed Co(0001) surface under pure CO (solid line) and under synthesis gas ($H_2$/CO = 2). This sequence shows the effect of varying the CO partial pressure and the sample temperature as follows: (a) $10^{-6}$ mbar/298 K, (b) ca. 5 mbar/298 K, (c) 100 mbar/298 K, and (d) 100 mbar/490 K.

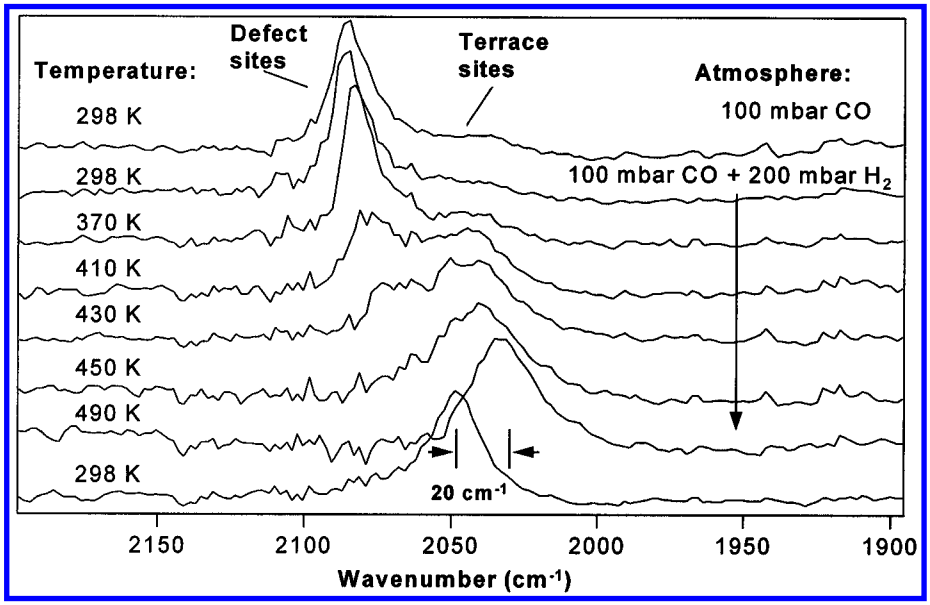


**Figure 2.** Sequence of PM-RAIR taken on a sputtered Co(0001) surface. The starting conditions were 100 mbar of CO at 298 K; 200 mbar of $H_2$ was then added and the temperature increased stepwise to 490 K. It can be seen that the absorption signal due to CO attached to defect sites is removed in an irreversible process.

Figure 2 shows another sequence of PM-RAIR spectra, this time for a sputtered Co(0001) surface. At 298 K under 100 mbar of pure CO, a complex absorption signal now occurs at ~2000−2100 $cm^{-1}$, composed of a sharp peak at 2080 $cm^{-1}$ and a smaller, broad peak at ~2020−2060 $cm^{-1}$. No significant change in the PM-RAIR spectrum is observed when an additional 200 mbar of $H_2$ is added to the RAIRS chamber at 298 K; i.e., at 298 K the PM-RAIR spectra under pure CO and under synthesis gas are once again almost identical.

The rest of the sequence shown in Figure 2 shows the effect of raising the temperature stepwise to 490 K under synthesis gas ($H_2$/CO = 2). Each spectrum was collected after holding the sample for 5 min at the indicated temperature. The sharp defect peak at 2080 $cm^{-1}$ shows a large decrease in intensity with increasing temperature, accompanied by a small shift to lower frequencies. At 490 K, the peak has totally disappeared. The peak at ~2020−2060 $cm^{-1}$ shows an increase in intensity with increasing temperature and is similarly accompanied by a shift to lower frequencies. At 490 K, the peak intensity approaches a more or less constant value. Lowering the temperature again to 298 K results in a shift in the terrace absorption signal to higher wavenumbers. The 2080 $cm^{-1}$ absorption signal, however, does not develop again, clearly showing the irreversibility of this process.

The temperature dependence of the signal intensities is given in more detail in Figure 3. Note that there is a sharp decrease in the defect signal which is accompanied by a sharp increase in the terrace signal above 370 K. This shows that not only is the 2080 $cm^{-1}$ species removed but also, at lower temperatures, that there is considerable transfer of intensity from the lower frequency terrace signal to the higher frequency defect signal, as also discussed elsewhere.[40] This means that the increase in intensity of the terrace signal with increasing temperature is not caused by an increasing CO coverage on the terraces but

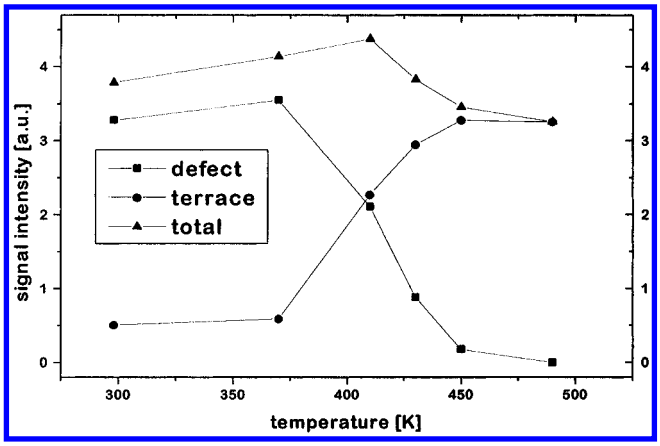


**Figure 3.** Integrated intensity of CO bonded to defects and to terraces and the total CO absorption intensity as a function of temperature. Data derived from Figure 2. The sharp decrease in the defect signal which occurs between 370 and 410 K is accompanied by a corresponding increase in the intensity of the terrace absorption signal. The total absorption intensity shows only a slight decrease.

by intensity transfer effects. At the same time, the *total* CO signal intensity in the frequency range 2000−2100 $cm^{-1}$ decreases slightly with increasing temperature.

In a third sequence of PM-RAIR spectra, a sputtered Co-(0001) surface was exposed to 100 mbar of CO, and then the temperature was raised to 490 K, resulting in the uppermost PM-RAIR spectrum shown in Figure 4. The sequence shows the effect of increasing $p_{H_2}$ stepwise at 490 K, while keeping the CO partial pressure constant. Each spectrum was collected after holding the conditions for 5 min at the indicated value of $p_{H_2}$ before proceeding to the following condition in the sequence; i.e., the spectra should again reflect the surface absorption layer close to steady state conditions for a given hydrogen partial pressure. The CO signal at ∼2080 $cm^{-1}$ first shows an increase with $p_{H_2}$ up to $p_{H_2} = 1$ mbar and subsequently decreases to zero intensity at $p_{H_2} = 100$ mbar. At the same time it broadens, which indicates that modified defect CO sites with lower absorption frequencies are created at hydrogen partial pressures between 1 and 50 mbar. At 50 mbar, peak decomposition shows a modified defect CO site with an absorption frequency of ∼2065 $cm^{-1}$ (inset). Note that this is again a red shift of about 20 $cm^{-1}$ compared to the defect signal at ∼2080 $cm^{-1}$. The CO signal centered at ∼2050 $cm^{-1}$ (linearly bonded CO at terrace sites) shows a sharp decrease in intensity with increasing $p_{H_2}$ up to $p_{H_2} = 1$ mbar and finally increases again with a maximum developing at 2040 $cm^{-1}$ and a pronounced shoulder on the low-frequency side.

In Figure 5, XPS spectra for the C(1s) and O(1s) regions after exposure to pure CO and after exposure to synthesis gas ($H_2$/CO = 2) are shown. For both types of treatment, the annealed (or sputtered) surface was heated up stepwise over a period of ∼1 h to 490 K. The sample temperature was then held constant at 490 K for 10 min before cooling the infrared cell to room temperature and pumping off prior to sample transfer back to UHV for XPS analysis. Three peaks can be resolved in the C(1s) region (Figure 5a) at 283.3, 284.4, and 285.9 eV which can be ascribed to $C^{ads}$ species (carbidic carbon), adsorbed hydrocarbon fragments, and molecularly adsorbed CO ($CO^{ads}$), respectively.[41] The coverages of the different carbon species dependent on the initial surface state (i.e., sputtered or annealed) and on the high-pressure treatment (i.e., CO or syngas) are summarized in Table 1.

After the high-pressure CO treatment both molecularly adsorbed CO and carbidic carbon, due to CO dissociation, are found. The sputtered surface is clearly more prone toward CO dissociation, as discussed previously.[40] After the high-pressure syngas treatment, however, in both cases (i.e., for both the annealed and sputtered surfaces) hydrocarbon species are dominant, showing that a FT reaction is taking place at the surface under these conditions. The total amount of carbide/hydrocarbons after high-pressure/high-temperature syngas treatment is in good agreement with previous studies[9] despite the factor of ∼3 difference in total pressure. However, the present results also show that after high-pressure CO/syngas treatment the major part of the cobalt surface is not covered by carbide/hydrocarbons but by molecularly adsorbed CO. This is in agreement with the large amount of molecularly adsorbed CO during and after the high-pressure/high-temperature (490 K) treatments which has been observed in this study by PM-RAIRS.

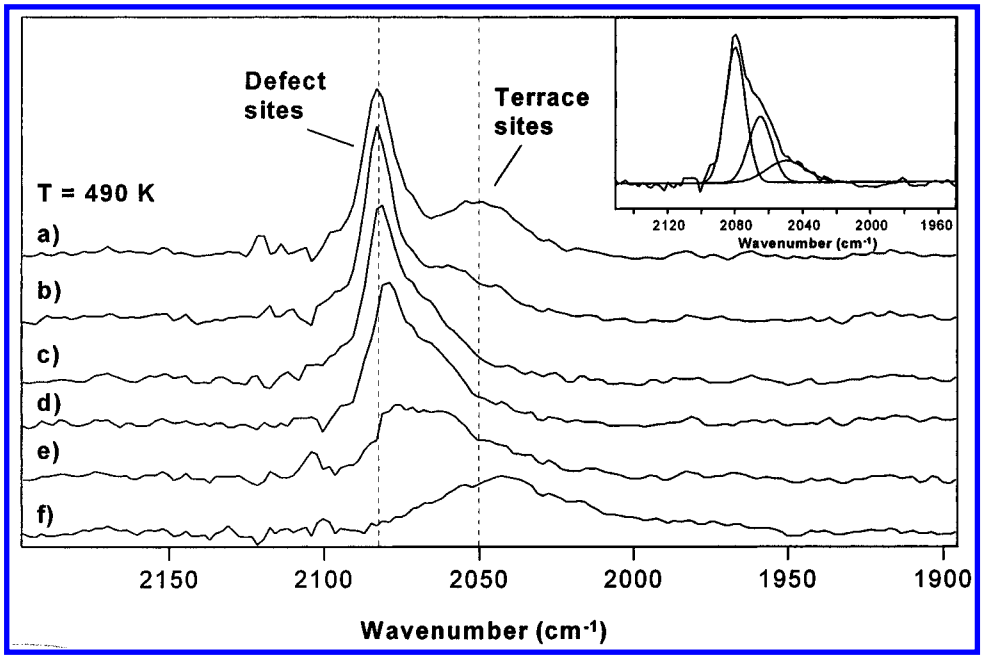


**Figure 4.** Series of PM-RAIR spectra taken on a sputtered Co(0001) surface. Starting conditions were 100 mbar of CO at 493 K (spectrum a). Then the hydrogen partial pressure was increased stepwise to (b) 1, (c) 5, (d) 10, (e) 50, and (f) 100 mbar. The "defect" CO signal at 2080 $cm^{-1}$ decreases sharply with increasing hydrogen pressure. At 10 mbar, a pronounced shoulder at 2065 $cm^{-1}$ develops (inset).

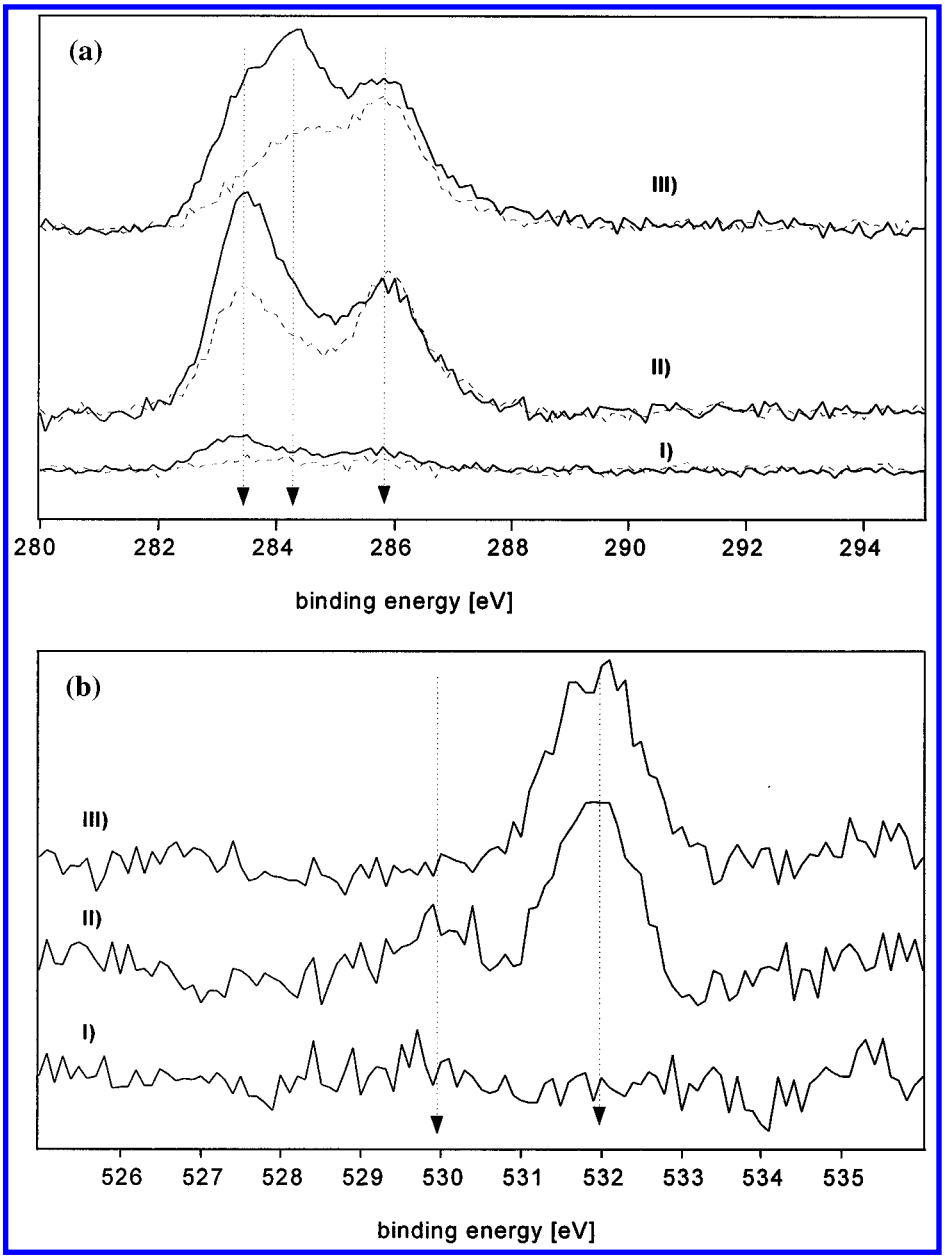


**Figure 5.** XPS plots showing (a, top) the C(1s) region for an annealed (dashed line) and a sputtered (solid line) Co(0001) surface after various treatments: (I) freshly prepared, (II) after 100 mbar of CO at 490 K, and (III) after 300 mbar synthesis gas at 490 K, and (b, bottom) the corresponding O(1s) region for the sputtered Co(0001) surface. Three carbon species can be distinguished: 283.3 eV (carbidic carbon), 284.4 eV (hydrocarbons), and 285.9 eV (adsorbed CO). Two oxygen species can be distinguished: 530 eV (adsorbed oxygen) and 532 eV (adsorbed CO).

**TABLE 1: Surface Coverages in % of a Monolayer (ML) Measured by *ex-Situ* XPS at Room Temperature for Different Carbon Species, Dependent on the Surface Preparation (Sputtering or Annealing) and on the High Pressure/High Temperature Treatment (CO or Syngas)**

| | annealed coverage (% of a ML) | | | sputtered coverage (% of a ML) | | |
|---|---|---|---|---|---|---|
| surface | carbide | hydrocarbons | CO | carbide | hydrocarbons | CO |
| freshly prepared surface | <1 | <1 | 1.2 | 3 | 2 | 3 |
| after 100 mbar of CO/490 K | 15.9 | 2.3 | 18.7 | 29.7 | 5.3 | 17.4 |
| after 300 mbar of syngas/490 K | 3.9 | 10.2 | 16.8 | 13.8 | 19.8 | 18.4 |

Inspection of the O(1s) region in XPS (Figure 5b) reveals no oxygen species after sputter treatment. After high-pressure CO treatment, however, two broader peaks can be discerned at 530 and 532 eV due to $O^{ads}$ and $CO^{ads}$, respectively.[41] The coverage of $O^{ads}$ is comparatively small (2−4% of a monolayer). These observations are in agreement with CO adsorption and partial dissociation as discussed above. High-pressure treatment in syngas leads to complete removal of the $O^{ads}$ species. These assignments are discussed in the next section in greater detail.

Figure 6 shows Anderson−Schulz−Flory (ASF)[2] plots for both annealed and sputtered Co(0001) during catalytic testing under flowing synthesis gas at 523 K, a total pressure of 1 bar ($H_2/CO = 2$), and a flow rate of 1 mL $min^{-1}$. The initial methanation activity of the sputtered surface exceeds that of the annealed surface by a factor of 10, while the initial $C_2^+$ activity is a factor of 5 higher. Only minor variations in the chain growth probability, $\alpha$, depending on pretreatment ($\alpha = 0.4-0.45$) are observed. For both the sputtered surface (solid

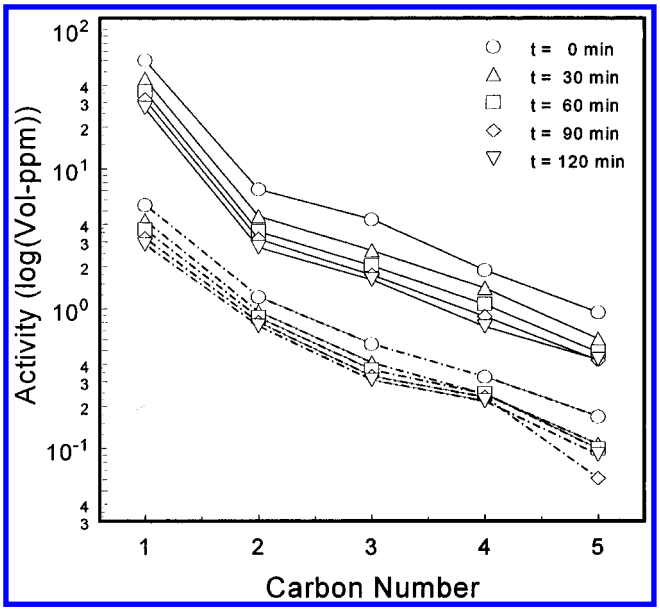


**Figure 6.** Anderson−Schulz−Flory plots of the sputtered (solid lines) and annealed (dotted lines) Co(0001) surface in the range $C_1-C_5$. The initial measurement has been repeated after 30, 60, 90, and 120 min and shows the deactivation behavior of this model catalyst.

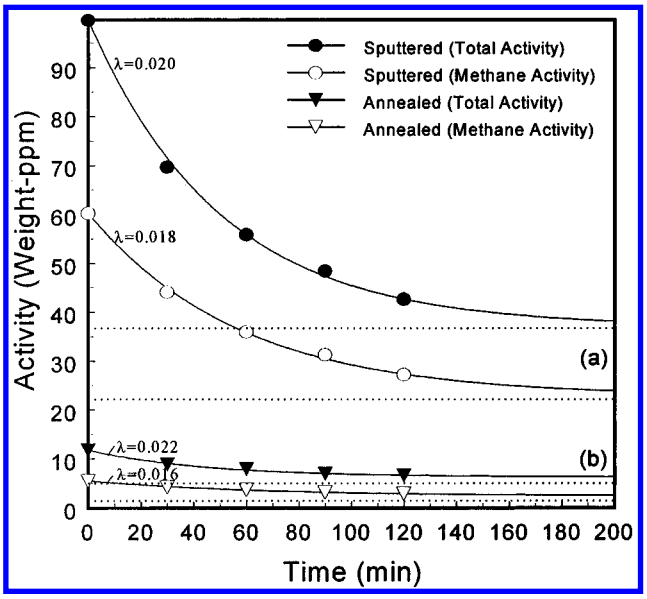


**Figure 7.** Plots showing the deactivation of both the total activity (all products summed) and the methane activity in greater detail for (a) the sputtered surface and (b) the annealed Co(0001) surface. The data are taken from Figure 6. The solid lines are fits to the data according to a simple first-order decay model of the form Activity($t$) = $Ae^{-\lambda t} + B$. In this model, $A$ and $B$ are fixed by the choice of $\lambda$ and the imposed requirement that the line passes exactly through the first ($t = 0$) and last ($t = 120$ min) data points. The only adjustable parameter is thus the decay constant, $\lambda$, which is given in each plot. Note that in each case the activity tends to a nonzero value ($=B$) indicated by the horizontal lines.

lines) and the annealed surface (dash-dotted lines), the deactivation behavior with time can also be seen. Figure 7 shows this deactivation behavior in more detail. The solid lines are corresponding fits to the data assuming simple exponential decay with time. The fitted decay exponent ($\lambda$) for each curve is given in the figure.

## 4. Discussion

**4.1. Coadsorption Behavior of CO and $H_2$ on Co(0001) at 298 K.** The PM-RAIR spectra taken at successively higher pressures under synthesis gas at 298 K are almost identical to the spectra taken under pure CO (Figure 1). For the case of pure CO, an explanation for the observed changes has been previously reported in greater detail elsewhere.[40] Briefly, a continuous compression of the CO adlayer occurs as $p_{CO}$ is increased. The structure of the CO adlayer changes from a $(\sqrt{3} \times \sqrt{3})R30°$ structure, with CO linearly bonded to "on-top" sites, to a closed packed $(2\sqrt{3} \times 2\sqrt{3})R30°$ structure, with CO located at both on-top sites and bridged sites. Both the frequency shifts and the changes in peak intensity of the on-top CO can then be explained in terms of coupling and depolarization effects[40] which are directly associated with these structural changes.

The similarity in the spectra obtained at 298 K under synthesis gas to the spectra obtained under pure CO shown in Figure 1 implies that a similar CO adlayer structure develops in both cases, which is insensitive to the presence of gas phase hydrogen. There are three obvious explanations for this apparent structure insensitivity. The first explanation is that the mixed $CO^{ads}/H^{ads}$ adlayer phase separates into separated $CO^{ads}$ and $H^{ads}$ domains. The second explanation is that the mixed adlayer does not phase separate but that any interaction between adjacent $CO^{ads}$ and $H^{ads}$ species at the surface is too small to be detected by PM-RAIRS. In both of these explanations, it is assumed that the surface is populated by similar coverages of $CO^{ads}$ and $H^{ads}$ species. The third explanation is simply that the hydrogen coverage is extremely low under these conditions; in this regime, a sharp distinction between phase separated domains or a homogeneous coadsorbed adlayer becomes difficult to establish experimentally.

It is known that on close-packed metal surfaces the CO−H interactions are repulsive in nature. This can be deduced from the observed formation of a segregated adlayer after dosing with mixtures of CO and $H_2$ at low temperatures (~100 K), e.g., on Rh(111) and Pt(111) surfaces.[42,43] At sufficiently high temperatures, however, segregation should not occur because of entropy effects.[17,42,44] In agreement with this, at 298 K we do not find any evidence for phase separation of the coadsorbed adlayer: the CO signal intensities at 298 K in PM-RAIRS do not change on going from a pure CO to a synthesis gas environment ($H_2/CO = 2$) in the pressure range $10^{-6} \leq p_{CO} \leq$ 100 mbar. Consider now the second explanation. This is also unlikely given the fact that $CO^{ads}$ and $H^{ads}$ have a repulsive interaction. These local repulsive interactions are certainly present, even at the higher temperatures used in the current experiments.[42,45] Even if entropy effects do preclude phase separation under these conditions, such repulsive interactions should nevertheless result in a marked shift in frequency of the CO absorption signal. For the case of CO/H coadsorption on Pt(111) surfaces under low-temperature conditions, a red shift in the CO absorption signal of 10−15 $cm^{-1}$ has been reported.[43] The small shifts in frequency observed in Figure 1a−c are of the same order of magnitude as the typical measurement error ($\pm 3$ $cm^{-1}$) in the absolute peak position found during repeat experiments. The most likely explanation for the current observations therefore, which is consistent with the fact that both the intensity as well as the frequency variations under pure CO and under synthesis gas are so similar, is that the $H^{ads}$ coverage under these conditions is very low.

This explanation is in agreement with low-temperature dosing experiments which show that close-packed metal surfaces are passivated by CO coverages >0.5 ML (a dense layer): as a result of the high CO coverage, the adsorption and subsequent dissociation of molecular hydrogen are severely inhibited.[17] In the current experiments, coverages in excess of 0.5 ML are certainly achieved in the 1−100 mbar regime, as can be seen

in Figure 1 with the appearance of an additional CO absorption signal due to bridge-bonded CO (only present at high CO coverages[40]). The identical spectra at room temperature obtained in 100 mbar of CO and 300 mbar of syngas and shown in Figure 2 show that the same conclusion with respect to the $H^{ads}$ coverage holds for the sputtered surface, too.

Further support for this explanation can be found in the coadsorption experiments of Bridge *et al.*[16] done at room temperature. In those experiments, TDS measurements have also revealed that the hydrogen atom coverage, after dosing a Co(0001) surface with a 1:1 mixture of $H_2$ and CO under UHV conditions, is very low. This was attributed to competitive adsorption due to the large difference in adsorption energy between adsorbed CO and dissociated hydrogen. It was also shown that preadsorbed hydrogen can be easily displaced by CO.

At lower CO coverages of 0.3 ML, however, quite open adlayers such as a $(\sqrt{3} \times \sqrt{3})R30°$ structure can exist. At low temperatures, it has been shown that $H_2$ can still undergo dissociation and coadsorb with CO.[17] The fact that we apparently do not see hydrogen adsorption at these lower coverages at room temperature suggests that $H_2$ pressures around $10^{-6}$ mbar are too low to produce a comparable steady state coverage at room temperature. This is reasonable since previous TDS experiments[16,44] have shown a desorption of hydrogen from clean Co(0001) and Ni(111) surfaces at temperatures (peak maximum) around 350−400 K, which is considerably lowered by 30−40 K in the presence of coadsorbed CO.

**4.2. Coadsorption Behavior of CO and $H_2$ on Co(0001) at 490 K.** Increasing the temperature in a pure CO atmosphere in the case of an annealed Co(0001) surface leads to a lower coverage of $CO^{ads}$, with an associated structural transformation from a $(2\sqrt{3} \times 2\sqrt{3})R30°$ structure back toward a $(\sqrt{3} \times \sqrt{3})R30°$ structure. This is the reason for the blue frequency shift and the increase in intensity of the linearly bonded CO signal seen in Figure 1 and has been discussed elsewhere.[40] From the intensity and frequency shift of the PM-RAIR spectra, a CO coverage between 0.33 and 0.5 ML under pure CO can be estimated by comparison with the spectra obtained at room temperature.[46] The comparable intensities under pure CO and under syngas at 490 K imply that the CO coverage under syngas is in the same range. This agrees with the observation that preadsorbed hydrogen can be easily displaced by CO rather than the other way round.[16]

The lower CO coverage at 490 K means that the surface layer is more open, which can be expected to favor $H_2$ adsorption and dissociation at high hydrogen partial pressures, resembling the low-pressure/low-temperature situation.[17] The frequency of the main CO absorption signal under synthesis gas is clearly shifted by about 20 $cm^{-1}$ to lower wavenumbers (a red shift) with respect to the signal obtained under 100 mbar of CO. This clearly demonstrates the influence of hydrogen on the CO adlayer at 490 K. It also agrees with the known activity of the Co(0001) single-crystal toward the Fischer−Tropsch reaction at this temperature.[9]

A likely explanation for this frequency shift is the formation of a nonsegregated, coadsorbed adlayer of $CO^{ads}$ and $H^{ads}$ in the high-temperature syngas atmosphere. Accordingly, we attribute the 20 $cm^{-1}$ shift to repulsive CO−H interactions, as reported previously on Pt(111) surfaces[43] and discussed above. These interactions completely offset the shift to higher wavenumbers due to structural changes which are observed in the case of pure CO upon increasing the temperature from 298 to 490 K. Nevertheless, the structural transition of the adsorbed CO layer under synthesis gas appears to be very similar to the transition observed under pure CO, as judged by the disappearance of the bridge-bonded CO species and the similar intensity increase of the main CO absorption signal.

A ∼20 $cm^{-1}$ red shift of the terrace absorption signal is also found for the sputtered surface at 490 K. Under pure CO at 490 K, the terrace absorption signal occurs at ∼2050 $cm^{-1}$ (peak maximum).[40] Under syngas at 490 K, it occurs at ∼2030 $cm^{-1}$ (Figure 2). In the case of the sputtered surface under pure CO, there are hardly any shifts in the peak positions on going from room temperature to 490 K,[40] indicating that structural changes in the CO adlayer are less pronounced.[47] This could be due to the larger defect density, which may relieve some of the compression of the terrace CO adlayer at room temperature, for example. If structural changes are no longer dominant, this implies that under syngas we should expect to see a ∼20 $cm^{-1}$ shift in the terrace absorption signal to *higher* frequencies, upon reducing the temperature from 490 to 298 K, due to the corresponding reduction in the surface coverage of $H^{ads}$. Figure 2 shows that this expectation is borne out. However, the situation is not quite so clear-cut. As a check, we also carried out an analogous blank experiment under pure CO (data not shown). This revealed a similar but smaller (∼10 $cm^{-1}$) shift to higher wavenumbers upon reducing the temperature from 490 to 298 K. Therefore, in the case of syngas, both repulsive CO−H interactions and dipole−dipole coupling effects are involved in the ∼20 $cm^{-1}$ shift seen in Figure 2. That dipole−dipole coupling effects are not evident for a freshly sputtered surface when the temperature is *increased* from 298 to 490 K under 100 mbar of pure CO most likely reflects the irreversibility of structural changes at the surface during annealing.

A similar red shift of the defect sites is also apparent in Figure 2 with increasing temperature and indicates that a *homogeneous* coadsorbed layer is formed at higher temperatures. In this case, however, the red shift is accompanied by a dramatic decrease in intensity. This is discussed further in the next section.

**4.3. Influence of Synthesis Gas on CO Bonded to Defects.** The behavior of the 2080 $cm^{-1}$ defect signal after annealing in a synthesis gas atmosphere is the central result of this paper. As reported earlier,[40] defects can be created by annealing a Co(0001) surface in a high-pressure CO environment or, in much higher concentrations, by directly roughening the surface by sputtering. As can be seen in Figure 1d, unlike the situation in pure CO, annealing in synthesis gas does not lead to the creation of a corresponding defect CO species. Moreover, the defect signal observed in the case of a sputtered surface under pure CO (as well as under synthesis gas) at 298 K completely vanishes during annealing in synthesis gas at 490 K, as can be clearly seen in both Figures 2 and 4.

Clearly then, the main change upon exposing a Co(0001) surface to synthesis gas at 490 K is the nonexistence or removal of the CO species adsorbed to defect sites. It has been shown elsewhere[25] that surface defects themselves are not removed during annealing under synthesis gas under similar conditions; on the contrary, just as in the case of annealing under pure CO, it is known for certain that defects are *created* during such a treatment. It follows that the disappearance of the CO defect signal must be due to the defect sites (which are still present) being unable to adsorb CO to a measurable extent under synthesis gas at 490 K.

In view of this we can envisage three possible explanations (only) for the disappearance of the defect CO signal. The first explanation is that $H^{ads}$ preferentially adsorbs at such sites and displaces defect CO. The second explanation is that the defect sites are simply blocked toward CO adsorption by individual C or O atoms (following CO dissociation at 490 K). The third

explanation is that CO is no longer able to adsorb at defect sites due to the formation of Fischer−Tropsch reaction products (i.e., growing hydrocarbon chains and/or $H_2O$) at these same sites. We now consider each explanation in turn.

The first explanation contradicts the experimental observations of a number of authors[16,17,42] which clearly show that CO displaces $H^{ads}$ from metal surfaces, rather than the other way around. A reversal of this effect at defects would require a switch in the relative *local* heats of adsorption of hydrogen and CO at defect sites. At low $H^{ads}$ coverages, the (spatially averaged) adsorption energy of hydrogen is known to approach that of CO which would support this local argument.[16] On the basis of Figure 2, however, we are able to rule out this argument altogether. Hydrogen is known to dissociate on metal surfaces, even at room temperature; it is a nonactivated process. Under synthesis gas, the CO defect signal in PM-RAIRS hardly changes throughout the temperature range 298−370 K. If the adsorption energy of hydrogen at defects were higher than that of CO, then no CO defect signal should occur in this temperature range either. The appearance of the defect signal therefore contradicts the proposed explanation.

The second explanation requires the blocking of all defect sites with either $C^{ads}$ or $O^{ads}$ atoms as a result of CO dissociation at the surface at 490 K. We have confirmed by XPS[40] in agreement with literature data[6] that CO dissociation does not occur to a significant extent at room temperature: after dosing a clean Co(0001) surface with 10 langmuirs of CO at 298 K, both the C(1s) and O(1s) regions show only one peak due to molecularly adsorbed CO, at binding energies of 285.9 and 532 eV, respectively. After annealing in pure CO at 490 K, two additional peaks appear at 283.3 and 530 eV, which can be assigned to the species $C^{ads}$ and $O^{ads}$ (Figure 5). After annealing in synthesis gas, the O(1s) 530 eV signal disappears completely. Therefore, a blocking effect due to $O^{ads}$ can be excluded. Most likely it is removed by $H^{ads}$ forming $H_2O$(g). The XPS data also allow a blocking effect due to $C^{ads}$ to be excluded: we observe considerably larger amounts of carbidic carbon after annealing in pure CO compared to annealing in synthesis gas (see Table 1); clearly, this larger amount under pure CO is not sufficient to block all the defect sites since we clearly observe a defect CO signal in PM-RAIRS under pure CO at high temperatures.

We are therefore led to the third explanation to account for our RAIRS data, namely, that CO is no longer able to adsorb at defect sites due to the formation of Fischer−Tropsch reaction products. We point out that we have not yet been able to detect peaks in PM-RAIRS associated with C−H or C−C vibrations which would provide direct proof for this statement. Nevertheless, XPS clearly shows an additional signal at 284.4 eV, following exposure to synthesis gas at 490 K, which can be assigned to adsorbed hydrocarbons,[41] in agreement with post-reaction EELS results previously obtained by Geerlings *et al*.[9] Consistent with the proposed explanation, in the case of the sputtered surface (high defect concentration) and the annealed surface (low defect concentration), the hydrocarbon XPS signal is found to dominate the entire C(1s) region. The sputtered surface, which contains the largest number of defects, also contains the largest number of hydrocarbons. Furthermore, it can be seen from Figures 2 and 3 that the CO defect signal shows a sudden decrease in intensity between 370 and 410 K. This closely matches with the known temperature at which the Fischer−Tropsch reaction starts to occur on Co(0001).[48]

Note that the line broadening apparent in Figure 4 as the defects are consumed (with increasing hydrogen pressure) more or less follows the same trend as Figure 2 (increasing temperature). Both trends can be explained in terms of a red shift of the defect sites with increasing $H^{ads}$ coverage. Interestingly, at intermediate hydrogen pressures, a clear separation of the total CO absorption signal into three distinct peaks is possible (see inset in Figure 4). The appearance of a distinct absorption signal at around 2065 $cm^{-1}$ suggests that the removal of CO attached to defect sites may proceed via a different CO defect species containing locally coadsorbed hydrogen and CO species.

Taken together, the *in-situ* RAIRS and *ex-situ* XPS data actually show that hydrocarbon molecules produced by the Fischer−Tropsch reaction are directly associated with the defect sites. This is a very striking conclusion to reach, since it strongly implies that the defect sites are the active sites for carbon chain growth in Fischer−Tropsch synthesis.[49] A similar conclusion was previously reached, on the basis of STM measurements, in a previous study.[25] In that *ex-situ* study, however, it was not possible to connect the observed formation of defects under synthesis gas with Fischer−Tropsch activity directly. The final experimental evidence confirming this conclusion is contained in the kinetic experiments discussed in the next section.

**4.4. Kinetic Measurements.** The kinetic data shown in Figures 6 and 7 show that the sputtered surface is more active in the FT reaction than the annealed surface. This is the case despite the occurrence of deactivation, which is found to be similar for both types of surface. In the absence of a detailed study, we refrain from discussing the reasons behind the deactivation. These kinetic measurements were carried out at 523 K, 1 bar total pressure, and a $H_2$/CO ratio of 2—the only difference compared to the 490 K RAIRS measurement shown in Figure 2 being a factor of 3 difference in total pressure and ∼30 K difference in temperature. Taken in combination with the RAIRS/XPS measurements discussed above, these measurements constitute direct evidence that defect sites are the active sites in Fischer−Tropsch synthesis over Co(0001). It is interesting to point out here that, despite the known occurrence of surface restructuring during FT synthesis,[25] Figure 7 shows that the number of active sites arrived at after several hours is strongly influenced by the defect morphology of the initial surface. One reason for this could be the influence of CO dissociation and carbide formation at defects, which then affects the subsequent course of surface restructuring (e.g., by step pinning) in this dynamic system.

## 5. Conclusions

The Fischer−Tropsch process has been studied for the first time *in-situ* at pressures and temperatures approaching industrial conditions on a Co(0001) single-crystal model catalyst using PM-RAIRS. By comparison with previous studies in a pure CO atmosphere,[40] the influence of synthesis gas ($H_2$/CO = 2) on the CO adsorption layer could be assessed. At room temperature (298 K), no influence of hydrogen on the CO adsorption could be observed, which was attributed to a very low $H^{ads}$ concentration at the surface. Under reaction conditions (490 K, $H_2$/CO = 2, 300 mbar total pressure), a ∼20 $cm^{-1}$ red shift in the CO absorption signal is observed due to the formation of a nonsegregated and homogeneous coadsorbed layer of CO and hydrogen, containing repulsive CO−H interactions. *In-situ* PM-RAIR spectra show that CO species attached to defect sites under high-pressure CO disappear under a syngas atmosphere at reaction conditions. It has been deduced that these sites are occupied by alkyl species. This conclusion has been checked by postreaction *ex-situ* XPS studies which revealed an enhanced hydrocarbon buildup on the sputtered surfaces. Furthermore, kinetic measurements showed a Fischer−Tropsch

activity which is enhanced by a factor of 5−10 on the sputtered surface compared to the annealed surface. This represents direct evidence that defects are the active sites for hydrocarbon synthesis in the FT process.

PM-RAIRS has emerged as a valuable tool in fundamental catalysis research which, in combination with conventional UHV surface preparation and surface analysis methods such as electron diffraction and electron spectroscopy, gives new insights into surface structure and surface processes of model catalysts under working conditions—particularly when combined with kinetic measurements. The investigation of the $CO/H_2/Co(0001)$ system is the first step in a series of model studies intended to probe the scope of PM-RAIRS for investigations in catalysis. Model surfaces closer to reality, such as polycrystalline metal surfaces exposing various low-index faces and grain boundaries or catalyst particles spin-coated on flat metal surfaces, where particle size effects and metal−support interactions are introduced, have been investigated as well.[50]

**Acknowledgment.** The authors thank E. W. Kuipers, G. J. Kramer, and H. P. C. E. Kuipers for helpful comments and valuable discussions.

## References and Notes

(1) Storch, H. H.; Golumbic, N.; Anderson, R. B. *The Fischer Tropsch and Related Syntheses*; Wiley: New York, 1951.
(2) Anderson, R. B. *The Fischer Tropsch Synthesis*; Wiley: New York, 1984.
(3) Iglesia, E.; Reyes, S. C.; Madon, R. J.; Soled, S. L. *Adv. Catal.* **1993**, *39*, 221.
(4) Hindermann, J. P.; Hutchings, G. J.; Kiennemann, A. *Catal. Rev.—Sci. Eng.* **1993**, *35*, 1.
(5) Bridge, M. E.; Comrie, C. M.; Lambert, R. M. *Surf. Sci.* **1977**, *67*, 393.
(6) Papp, H. *Surf. Sci.* **1983**, *129*, 205.
(7) Greuter, F.; Heskett, D.; Plummer, E. W.; Freund, H. J. *Phys. Rev. B* **1983**, *27*, 7117.
(8) Lahtinen, J.; Vaari, J.; Talo, A.; Vehanen, A.; Hautojärvi, P. *Vacuum* **1990**, *41*, 112.
(9) Geerlings, J. J. C.; Zonnevylle, M. C.; Groot, C. P. M. de *Surf. Sci.* **1991**, *241*, 302.
(10) Prior, K. A.; Schwaha, K.; Lambert, R. M. *Surf. Sci.* **1978**, *77*, 193.
(11) Prior, K. A. *PhD Thesis*, Cambridge University, Cambridge UK, 1979.
(12) Geerlings, J. J. C.; Zonnevylle, M. C.; Groot, C. P. M. de *Surf. Sci.* **1991**, *241*, 315.
(13) Papp, H. *Surf. Sci.* **1985**, *149*, 460.
(14) Papp, H. *Ber. Busen-Ges. Phys. Chem.* **1982**, *86*, 555.
(15) Toomes, R. L.; King, D. A. *Surf. Sci.* **1996**, *349*, 1.
(16) Bridge, M. E.; Comrie, C. M.; Lambert, R. M. *J. Catal.* **1979**, *58*, 28.
(17) White, J. M.; Akhter, S. *Crit. Rev. Solid State Mater. Sci.* **1988**, *14*, 131.
(18) Schlögl, R. *Angew. Chem.* **1993**, *105*, 402.
(19) Campbell, C. T. *Adv. Catal.* **1989**, *36*, 1.
(20) Ertl, G. *Angew. Chem.* **1990**, *102*, 1258.
(21) Goodman, D. W.; Kelley, R. D.; Madey, T. E.; Yates Jr., J. T. *J. Catal.* **1980**, *63*, 226.
(22) Kelley, R. D.; Goodman, D. W. In *The Chemical Physics of Solid Surfaces and Heterogeneous Catalysis*; King, D. A., Woodruff, D. P., Eds.; Elsevier: Amsterdam, 1982; Vol. 4, Chapter 10.
(23) Bonzel, H. P.; Krebs, H. J. *Surf. Sci.* **1980**, *91*, 499.
(24) Bonzel, H. P.; Krebs, H. J. *Surf. Sci.* **1982**, *117*, 639.
(25) Wilson, J. H.; Groot, C. P. M. de *J. Phys. Chem.* **1995**, *99*, 7860.
(26) Yates, J. T.; Worley, S. D.; Duncan, T. M.; Vaughan, R. W. *J. Chem. Phys.* **1979**, *70*, 1225.
(27) Kruse, N.; Gaussmann, A. *J. Catal.* **1993**, *144*, 525.
(28) Jong, A. M. de; Niemantsverdriet, J. W. *J. Chem. Phys.* **1994**, *101*, 10126.
(29) Hoffmann, F. M.; Robbins, J. L. *J. Electron Spectrosc. Relat. Phenom.* **1987**, *45*, 421.
(30) Weisel, M. D.; Robbins, J. L.; Hoffmann, F. M. *J. Phys. Chem.* **1993**, *97*, 9441.
(31) Hoffmann, F. M. *J. Chem. Phys.* **1989**, *90*, 2816.
(32) Peden, C. H. F.; Goodman, D. W.; Weisel, M. D.; Hoffmann, F. M. *Surf. Sci.* **1991**, *253*, 44.
(33) Glass, A. S.; Bermudez, V. M. *J. Vac. Sci. Technol. A* **1990**, *8*, 2622.
(34) Burrows, V. A.; Sundaresan, S.; Chabal, Y. J.; Christman, S. B. *Surf. Sci.* **1987**, *180*, 110.
(35) Laskov, A.; Beitel, G. A.; Oosterbeek, H.; Kuipers, E. W. To be published.
(36) Golden, W. G.; Saperstein, D. D. *J. Electron Spectrosc. Relat. Phenom.* **1983**, *30*, 43.
(37) Golden, W. G.; Saperstein, D. D.; Severson, M. W.; Overend, J. *J. Phys. Chem.* **1984**, *88*, 575.
(38) Nafie, L. A. In *Advances in Applied Fourier Transform Infrared Spectroscopy*; Mackenzie, M. W., Ed.; Wiley: London, 1988; p 67.
(39) Buffeteau, T.; Desbat, B.; Turlet, J. M. *Appl. Spectrosc.* **1991**, *45*, 380.
(40) Beitel, G. A.; Laskov, A.; Oosterbeek, H.; Kuipers, E. W. *J. Phys. Chem.* **1996**, *100*, 12494.
(41) Moulder, J. F.; Stickle, W. F.; Sobol, P. E.; Bomben, K. D. *Handbook of X-Ray Photoelectron Spectroscopy*; Perkin-Elmer: Eden Prairie, MN, 1992.
(42) Williams, E. D.; Thiel, P. A.; Weinberg, W. H.; Yates, J. T. *J. Chem. Phys.* **1980**, *72*, 3496.
(43) Hoge, D.; Tüshaus, M.; Bradshaw, A. M. *Surf. Sci.* **1988**, *207*, L935.
(44) Peebles, D. E.; Creighton, J. R.; Belton, D. N.; White, J. M. *J. Catal.* **1983**, *80*, 482.
(45) Haq, S.; Love, J. G.; King, D. A. *Surf. Sci.* **1992**, *275*, 170.
(46) It has been shown by Goodman *et al.* for the system CO/Cu(100) that isosteric heats of adsorption measured at low pressures and low temperatures can be extrapolated remarkably well into the high-pressure regime.[51,52] Extrapolating the low-pressure data of Papp[6] obtained from work function measurements to the high-pressure regime, the CO adsorption energy corresponding to the CO coverage range and conditions under which Figure 1d was measured (490 K, $p_{CO} = 100$ mbar) can be estimated to be 100 kJ/mol.
(47) In particular, no bridge-bonded CO species are formed implying that the terrace adsorbed CO overlayer does not proceed beyond a $(\sqrt{3} \times \sqrt{3})R30°$ structure.
(48) Henrici-Olivé, G.; Olivé, S. *Angew. Chem., Int. Ed. Engl.* **1976**, *15*, 136.
(49) We should point out here that we are unable to distinguish between adsorbed $CH_3$ species and longer hydrocarbon fragments on the basis of our XPS measurements. Direct evidence for *growing* hydrocarbon chains is contained in the kinetic measurements shown in Figures 6 and 7.
(50) Riedmüller, B.; Beitel, G. A.; Oosterbeek, H.; Kramer, G. J. To be published.
(51) Truong, Ch. M.; Rodriguez, J. A.; Goodman, D. W. *Surf. Sci. Lett.* **1992**, *271*, L385.
(52) Kuhn, W. K.; Szanji, J.; Goodman, D. W. *Surf. Sci. Lett.* **1992**, *274*, L611.